10^{th} International Conference on Fracture Mechanics of Concrete and Concrete Structures
FraMCoS-X
G. Pijaudier-Cabot, P. Grassl and C. La Borderie (Eds)
https://doi.org/10.21012/FC10.235532

FRACTURE BEHAVIOUR OF ULTRA-HIGH PERFORMANCE CONCRETE

AWADHESH SHARMA*, SONALISA RAY† AND MOHD. ASHRAF IQBAL‡

* Research Scholar, Indian Institute of Technology Roorkee
Roorkee, India
e-mail: awadheshced.dce2017@iitr.ac.in

† Assistant Professor, Institute of Technology Roorkee
Roorkee, India
e-mail: sonarfce@iitr.ac.in

‡ Associate Professor, Indian Institute of Technology Roorkee
Roorkee, India
e-mail: iqbalfce@iitr.ac.in

Key words: UHPC, Flexural Performance, Fracture Properties, Ductility

Abstract. In this work, an attempt has been made to develop and investigate mechanical and the fracture behaviour of ultra-high performance concrete (UHPC). Geometrically similar notched beam specimens of different sizes made up of ultra-high performance fibre reinforced concrete (UHPFRC) have been considered for the experimental investigation. Centre point bending tests have been performed on beam specimens in crack mouth opening displacement control manner for investigating the fracture properties. Various fracture properties such as, fracture toughness, fracture energy, brittleness number etc. have been determined on the basis of non-linear fracture mechanics theory. The results of UHPC concrete have been compared with that of normal strength concrete available in the literature. It has been observed that addition of fibres increases the energy absorption capacity to a great extent for all size of specimens of ultra-high performance concrete as compared to normal concrete. Moreover, the brittleness number has been found to decrease due to the addition of fibers thereby enhancing the ductility. A decrease in nominal strength of UHPC based concrete with the increase in specimen size has been observed in similar fashion as normal strength concrete. However, the sensitivity to the size effect of ultra-high performance concrete is effectively reduced compared with normal concrete.

1 INTRODUCTION

Ultra high performance concretes (UHPC) is characterized high strength, workability and improved durability properties. Well established high strength concrete (HSC) is characterized by only high compressive strength. With the use of reinforced fibers (steel fibers, glass fibers etc.), tensile and flexural of such highly brittle materials can be enhanced considerably. Poor fracture properties of UHPC has given scope to characterize its fracture properties [15, 18]. When the fiber and matrix parameters are properly selected, the addition of fibers can improve the fracture energy (G_f) of such ultra-high-performance fiber reinforced concretes (UHPFRC) considerably developing significant interest for practical applications. Fracture energy is influenced by numerous variables which include the fiber and matrix properties, their bond behavior, and the average num-

ber and inclination of fibers crossing the crack.

2 LITERATURE REVIEW

Recent industrial demands for new and excellent construction materials leads the development of new advanced cementitious materials. One of them is ultra-high performance concrete (UHPC) having high strength, high durability, and good workability [1], is still in the emerging stage. Using conventional natural and manufactured fine aggregates including ground granulated slag, it is possible to produce concrete with good workability and high compressive strength in the range of 130-160 MPa without special mixing or curing process [5]. The mechanical properties of UHPC include compressive strength greater than 120 MPa and sustained post-cracking tensile strength greater than 5 MPa [2]. According to previous study [4], UHPC exhibits less ductile behavior compared to high ductile fiber reinforced normal strength grade cementitious composites when the same amount of fiber is incorporated. Typical UHPC contains 2 % volume of steel fibers, whereas, high ductile fiber-reinforced normal strength grade cementitious composites presenting excellent tensile strain capacity of more than 2 % includes PVA (polyvinyl alcohol) or PE (polyethylene) fibers in general [6, 7]. Hardening post-cracking behavior achieved through the intensive use of discontinuous short steel fibers [9]. Addition of short, discontinuous steel fibers greatly enhances the flexural and shear behaviors of UHPC beams compared to non-fiber-reinforced specimens [16, 17]. Intensive research has been conducted to investigate the effect of curing regime on the mechanical properties of UHPC [8]; however, limited studies have found on comprehensive investigation on the effect of mixture proportions considering locally available materials. Yu et al. [13] investigated the effect of mixture design of UHPC with densely compacted cementitious matrix on the workability, air content, porosity, and compressive and flexural strengths. Three UHPC mixtures have been developed with cement content of 875 (kg/m^3) with 30% and 20% cement replacement with limestone and quartz. In addition, different ratios of steel fibers have been investigated ranging from 0.5 to 2.5% by volume of concrete. The study showed that the highest compressive strength (approximately 150 MPa) and flexural strength (approximately 30 MPa) were achieved with 2.5% steel fiber content. However, mixtures with limestone and quartz replacement showed enhanced workability and flow-ability. Magureanu et al. [11] has been presented compressive strength up to 183 MPa and flexural strength up to 30 MPa for 2.55 Vol.-% hybrid steel fibres reinforcement. Concrete strength increases in proportion with the fibres addition for fibres volumes up to 2.55%. The fibres considerably improved the concrete ductility and energy absorption capacity. The fracture energy exceeded 20000 N/m for 2.55 Vol.-% fiber reinforced concrete.

The addition of steel fibers to UHPC matrices successfully increased the fracture toughness, tensile strength, ductility and energy absorption capacity of UHPCs, although their performance were various according to the types of fiber. Park et al. [12] has been reported the direct tensile behavior of UHPC. The authors reported relatively high tensile strength (18 MPa), strain capacity (0.6%) and tiny multiple micro cracks lower than 20 mm crack width by blending only 1% long deformed and 1.5% short smooth steel fibers together. Ultra-high performance concrete with no fibers and high performance concrete don't generally exhibit high fracture toughness compared to normal strength concrete due to their intrinsic brittleness, in spite of high compressive strength. The flexural tensile strength of ultra-high performance steel fibre reinforced concrete (UHPFRC) linearly increases as the fiber volume ratio increases from 0% to 5% and the rule of mixture holds for the flexural strength of UHPFRC [14]. The increase of UHPFRC's tensile strength is promoted by factors which influence fibers efficiency, such as: fibers' geometric properties, volumetric ratio and bond characteristics. Use of deformed fibers and increasing fiber content greatly enhanced the peak

load under flexure and the flexure toughness characteristics of UHPC. According to Aziz et. al. [10] the fracture energy of UHPC could reach more than six times that of the normal-strength concrete. Accordingly, this study examines experimentally the tensile fracture properties of UHPC and fracture parameters were determined to compare with the normal concrete (NC) from the literature [3]. A wide range of experimental studies is required to investigate the fracture parameters and size effect studies of UHPC. In order to promote the applicability of UHPC structures, it is necessary to first develop in accordance to the mechanical characteristics of UHPC. However, despite the recent efforts to find out the mechanical behaviors of UHPC, a lack in this experimental investigation for quantitative assessment of fracture parameters in structural members are currently lacking.

3 EXPERIMENTAL PROGRAM

3.1 Materials and Mix proportions

The mix design of ultra-high performance fiber reinforced concrete (UHPFRC) differs significantly from that of normal and high-strength concrete. In this study, UHPFRC mix compositions are characterized by high cement content, fine aggregates, superplasticizer, fly-ash, quartz powder and steel fiber. Materials used for mix design of UHPFRC are given in Table 1. Mixture design is a selection of raw materials in optimum proportions to give concrete with required properties in fresh and hardened states for particular applications. The design of UHPFRC aims to achieve a densely compacted cementitious matrix with good workability and strength and durability properties. To achieve the required workability and mechanical properties, several trials with different combinations of materials have been done with and without steel fibres. Modified Andreasen and Andersen model [20] has been used as a target function for the optimization of the composition of mixture of granular materials. The concrete mixture proportions used in this study are tabulated in Table 2. The water–binder ratio $(\frac{w}{b})$ is determined as 0.175. Percentage of fly-ash and quartz powder used in the mix design are as 20% and 10% of cement weight, respectively. Quartz powder is used as siliceous filler. Furthermore, in order to increase flexural properties and achieve sufficient strain-hardening behavior, hooked end steel fibers 2.5% were incorporated. MasterGlenium 51-Polycarboxylic ether (PCE) based superplasticiser has been used. It reduces water content by more than 35% and helps to achieve very high early strength. Assuming air entrainment negligible, chemical admixture taken is 3% of weight of binder content.

Table 1: Material used and their specifications

Material	Specification
Ordinary Portland cement	As describe in IS: 12269, specific gravity = 3.15
Fly ash	Grey, confirming to IS: 3812 (Part1) 2013, Specific gravity = 2.22
Fine aggregate	Locally available river sand Zone 2 confirming to IS: 383- 1970 (particle size range of 0.6 mm-4.75 mm)
Quartz powder	white, 20-micron average particle size, 99% silica content,specific gravity = 2.65
Superplasticiser	Master Glenium 51- PCE, confirming to ASTM C494
Steel fiber	Hooked end carbon steel fiber with 30 mm length and 0.6 mm diameter, strength of steel fiber = 1400 MPa

Table 2: Composition of UHPFRC

Constituent	Quantity (kg/m^3)
Cement	872
Fly ash	248
Fine aggregate	925
Quartz powder	124
Superplasticiser	37*
Steel fiber	196.25
Water	217.7*

* in liter

3.2 Specimen details

For determination of fracture parameters, geometrically similar beams of three different sizes with the pre-notching have casted. Mixing and casting of UHPFRC is a complex process and precautions should be taken during casting procedure. Initially, fine aggregate is added into mixture followed by cement, fly ash and quartz powder and a low mixing is allowed for 5 minutes. Initially the mixing is done with 70% of water followed by addition of superplasticizer and remaining water with high speed mixing. Steel fibers are added when proper flowable UHPC cement obtained. Casting of concrete is generally completed quickly to avoid evaporation loss of water and moulds are covered with plastic sheets to avoid initial water loss to minimize drying shrinkage. The exposed surface of the mould were covered with wet burlaps until the surface becomes hard enough. Beam samples are further put into water after 2 days for curing at room temperature. Notch-depth ratio of beam specimens is kept as 0.2. The details of the geometry and its nomenclature of the beams are shown in Figure 1 and Table 3, respectively.

Table 3: Dimensions of beams

Parameters	Small	Medium	Large
Span, S (mm)	188	375	750
Depth, d(mm)	75	150	300
Thickness, b (mm)	75	75	75
Notch depth	15	30	60

Figure 1: Geometrically similar beam specimens.

3.3 Testing procedure

For the determination of fracture parameters three point bending test is performed on MTS DuraGlide servo hydraulic actuator (a closed loop servo-controlled testing machine having a capacity of 250 kN). Centre point notched beam specimens were recommended to be used according to the RILEM technical committee 89-FMT [21]. The support and loading arrangement is such that the forces acting on the beam are statically determinate. The test is performed in CMOD controlled manner with a rate of $(0.001mm/sec)$. This allows the maximum load to be reached within about 90-180 seconds after the start of the test depends upon the specimen size. A relationship between the load-CMOD and load-displacement is recorded during entire test run. The CMOD measurements were obtained using a cantilever type clip gauge connected to flex test Conditioner. The load point displacements were recorded through LVDT. The compliance is determined from initial portion of load–CMOD curve. Determination of fracture parameters is following work-of fracture and size effect law method.

4 RESULTS AND DISCUSSIONS

4.1 Initial properties of UHPC

Fresh properties of UHPC are as important as its hardened properties. To evaluate fresh properties of concrete workability was found out using flow table method which is genrally preferred for higher workable concrete having slump value more than 175 mm. For workability, a square flow table of 900 mm size was used and a cone similar to conventional slump testing was filled upto top layer. Concrete was allowed to expand on the flow table, and its diameter was measured and the flow diameter is average of the maximum diameters measured. It was observed that addition of steel fibers resist flow of UHPFRC compared to UHPC without fibers. The observed slump flow was 665 mm with steel fibers wherein, a slump of 855 mm was observed in case of without steel fibers. Similarly, slump flow values of 18 sec and 10 sec were observed in the presence of steel fibers

and absence of fibers.

4.2 Mechanical Properties

After obtaining the fresh properties, specimens namely cubes UHPC and UHPFRC were cast for mechanical properties considering both with and without fibers. Concrete cubes of dimension 150 mm $\times$ 150 mm $\times$ 150 mm were cast and moist cured for 28 days. The compression testing of concrete cube was performed as per IS 516 [23]. Cylinder of 100 mm dia. and 200 mm height were cast and tested for split tensile strength as per IS 516 [23]. Flexural strength of concrete was measured by testing of beam of size 100 mm $\times$ 100 mm $\times$ 500 mm under four point bending test using digital universal testing machine by applying load at 1/3rd of the support span. The results of compression test, split tensile strength and flexural strength of UHPFRC and UHPC are presented in Table 4. Modulus of elasticity (E_c) of UHPFRC was calculated as 42153 MPa experimentally which is used in the fracture parameters determination.

Table 4: Hardened properties of UHPFRC and UHPC

Concrete type	Compessive strength (MPa)	Split Tensile strength (MPa)	Flexural strength (MPa)
UHPFRC	143.67	12.74	20.95
UHPC	128.50	9.65	14.84

Upon addition of hooked end steel fibers in UHPC, 28 days compression strength is enhanced by 11.80%. Fibers lead to nominal increase in compressive strength and nominal increase in split tensile strength and flexural strength. Split tensile strength was increased by 64.47% while flexural strength was increased by 68.12% with the addition of steel fibers in UHPC. Therefore, for the subsequent studies, only UHPFRC i.e. including fibres have been considered.

4.3 Fracture parameters

Testing on notched concrete beam specimens was conducted on closed loop servo-controlled testing machine under crack mouth opening (CMOD) control at an opening rate of 0.001 mm/s. The results of variation of load with CMOD and the mid-span vertical displacement acquired during the test were analyzed to obtain various fracture parameters. The static tests were run until the maximum opening of the clip guage i.e. 4 mm. For small, medium and large specimens, average maximum loads were recorded as 15.92 kN, 28.74 kN and 44.57 kN respectively for UHPFRC.

Table 5: Peak load of geometrical similar beams in kN

Type of concrete	Small	Medium	Large
Normal concrete	2.35	3.97	6.38
UHPFRC	15.92	28.74	44.57

It can be observed that the peak load, displacement and the critical crack opening displacement values increases with the increase in specimen size for both normal concrete and UHPFRC. Variation of load with crack mouth opening displacement for both normal concrete (NC) and UHPFRC are presented in Figure 2 and Figure 3 respectively. For better understanding, the peak load values for small, medium and large size specimen in both the types of concrete are presented in Table 5.

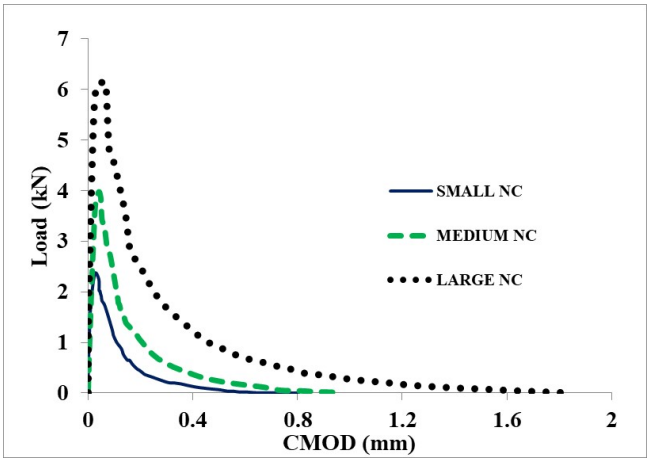

Figure 2: Variation of load with CMOD (NC) [3].

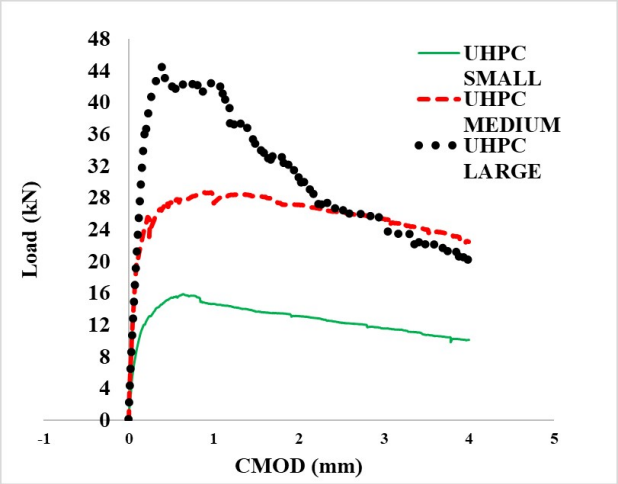

Figure 3: Variation of load with CMOD (UHPFRC).

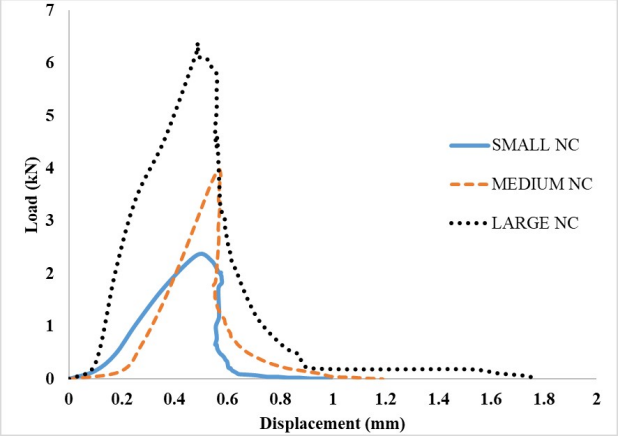

Figure 4: Variation of load with displacement (NC).

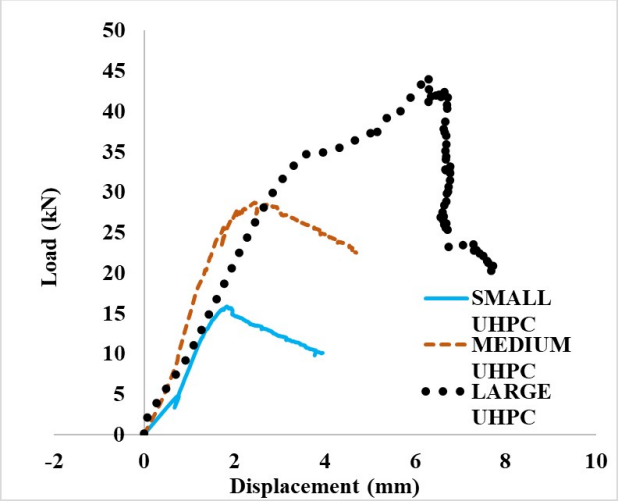

Figure 5: Variation of load with displacement (UHPFRC).

Further, variations of load with load point vertical displacement for normal concrete and UHPFRC specimen have been plotted in Figure 4 and Figure 5, respectively . It can be observed that the energy absorption capacity is increased considerably with the addition of fibres.

The fracture energy is defined as the amount of energy necessary to create a crack of unit surface area projected in a plane parallel to the crack direction. Based on measured load-deflection curve of a three point bend notched beam, the work of load P on the load-deflection δ in RILEM method is calculated as $W_f = \int P d\delta$ The fracture energy G_F according to the RILEM [19] definition,

$$G_F = \frac{W_f}{B[(1-\alpha_0)d]} \tag{1}$$

where $\alpha_0 = \frac{a_0}{d} = 0.2$, initial notch to depth ratio. From Table 6, fracture energy (G_F) was calculated as 10.31 N/mm, 9.06 N/mm and 6.86 N/mm for small, medium and large specimens respectively. A decrement of 12.21% and 33.46% was observed for medium and large specimens with respect to small specimen. It can be observed that energy absorption capacity is higher for small specimen as compared to medium and large specimens. Furthermore, in the linear fracture mechanics (LEFM), the fracture toughness for mode I, also called the critical stress intensity factor, is generally calculated from:

$$K_{Ic} = \sigma_N \sqrt{\pi . a_c} f(\alpha_0) \tag{2}$$

in which σ_N is the nominal failure stress, $\alpha = \frac{a}{d}$, $f(\alpha)$ is dimensionless function and a is initial crack length. For Span/depth ratio= 2.5, the geometric function $(f\alpha)$ is expressed as [25]:

$$f_{(\alpha)} = \frac{1.83 - 1.65\alpha + 4.76\alpha^2 - 5.3\alpha^3 = 2.51\alpha^4}{(1+2\alpha)(1-\alpha)^{\frac{3}{2}}} \tag{3}$$

The fracture toughness (K'_{Ic}) has been calculated using fracture energy (G_F) from work of fracture method and the Young's modulus E following LEFM approach as below:

$$K'_{Ic} = \sqrt{G_F . E} \tag{4}$$

Table 6: Fracture energy G_F, K_{Ic} and K'_{Ic} for different size of specimens

Specimen type	$G_F(\frac{N}{mm})$	K'_{Ic} $(MPa\sqrt{m})$	K_{Ic} $(MPa\sqrt{m})$
Small	10.31	20.84	15.68
Medium	9.06	19.54	13.87
Large	6.86	17.00	11.96

The quantity fracture toughness K_{Ic} is obtained based on the ultimate load on the ascending branch of a load-displacement curve, including linear loading and hardening and can be used to reflect the resistance of concrete against cracking. However, it cannot represent the crack resistance of the concrete over the whole loading process because it neglects the resistance after the peak load, i.e. softening property. Stiffness change and fracture energy can be collectively used to describe the fracture toughness of concrete (K'_{Ic}) which can represent the behavior of concrete at both ascending and descending branches of the complete loading process including linear, hardening and softening.

From Table 6, it can be observed that K'_{Ic} and K_{Ic} decreased on increasing the size of the beam and a decrease of 6.23 % and 18.42% was observed for medium and large specimens respectively when compared to small specimens. The ratios $(\frac{K'_{Ic}}{K_{Ic}})$ were obtained as 1.32, 1.41, 1.42 respectively, for small, medium and large specimens. These ratios imply that the contributions from softening portion of the load-displacement curve in crack resistance in UHPFRC are comparatively smaller than the contributions from the ascending portion of the curve.

K_{Ic} is an instantaneous parameter and represents the cracking resistance at the peak load, while K'_{Ic} is a more synthetic process parameter and represents the resistance over the whole fracture process. Thus from the results we can conclude that cracking resistance for UHPFRC is mostly governed by the linear and hardening portions of the stress-strain curve.

The fracture parameters viz. material fracture energy (G_f), effective length of fracture process zone (c_f) were obtained using Size effect law proposed by Bazant [19].

$$\sigma_N = \frac{Bf_t}{\sqrt{1+\beta}} \tag{5}$$

Where, $\sigma_N = c_n \frac{P_u}{bd}$ is nominal strength of two-dimensional similar structures, $\beta = \frac{d}{d_0}$ is the brittleness number, B and d_0 are empirical constants, f_t is the material tensile strength, c_n is a coefficient introduced for convenience, P_u is the ultimate load, b is the specimen thickness, and d is the characteristics specimen size (i.e., depth of the beam).

Fracture parameters were determined using size effect model [19] by testing geometrically similar specimen under three point bending loading test. Linear regression analysis was carried out as shown in Figure 6 by arranging a plot of X = d and Y = $(\frac{1}{\sigma_N})^2$ and a linear equation may be found as Y = AX + C. Where, A is slope of regression line and C is intercept on Y-axis, evaluated from the regression plot as regression constants Bf_t and d_0 were calculated as $Bf_t = \frac{1}{\sqrt{C}}$ and $d_0 = (\frac{C}{A})$ For known values of relative crack length, $\alpha = \frac{a}{d}$, S/d =2.5

The value of Bf_t and transition size in size effect law (d_0) were obtained as 3.312 MPa and 168.75 mm respectively. $F(\alpha)$ is function of relative crack length and it can be calculated by following equation:

$$F(\alpha) = \frac{1.0-2.5\alpha+4.49\alpha^2-3.98\alpha^3+1.33\alpha^4}{(1-\alpha)^{\frac{3}{2}}} \tag{6}$$

The non-dimensional function which characterizes the geometry of the structure $g(\alpha)$ can be determined by using the Handbook [24]

$$g(\alpha) = \left(\frac{S}{d}\right)^2 \pi\alpha[1.5F(\alpha)] \tag{7}$$

For $\alpha_0 = a_0/d$ = initial crack length, $g(\alpha = \alpha_0)$ was calculated.
The material fracture energy G_f was calculated using the following expression:

$$G_f = \frac{g(\alpha_0)}{E_c A} \tag{8}$$

Where E_c is modulus of elasticity of concrete.

$$c_f = \frac{g(\alpha_0)}{g'\alpha_0)}\left(\frac{C}{A}\right) \tag{9}$$

where $g'(\alpha) = \frac{dg(\alpha)}{d\alpha}$ and equation 9 is valid only if $g'(\alpha) > 0$.

The fracture toughness according to the size-effect law K_{Ic} is easy to evaluate using the LEFM relationship $K_{Ic} = \sqrt{G_f E}$. For the present study, values of material fracture energy (G_f), effective length of fracture process zone (c_f) were obtained as 3.39 N/mm, 45.03 mm respectively. The ratio of average fracture energy (G_F) calculated using work of fracture method to that of material fracture energy calculated using size effect model has been obtained and is presented in Table 7. For all the sizes of beams under study, the ratios obtained were greater than 2.0.

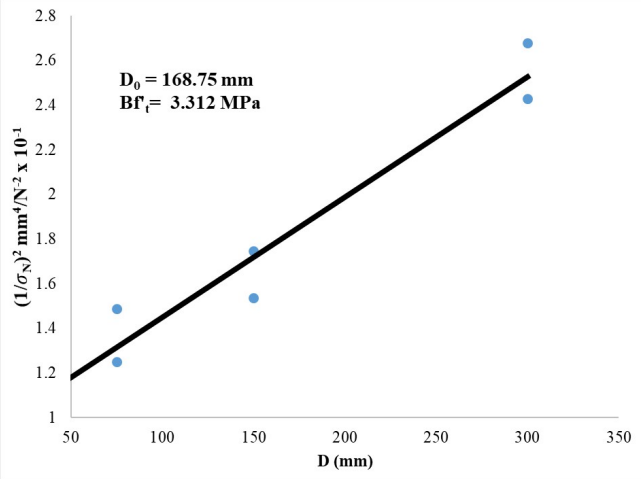

Figure 6: Linear regression plot constructed from the maximum load values

Table 7: Fracture energy ratio $(\frac{G_F}{G_f})$

Specimen type	$G_F(\frac{N}{mm})$	Ratio of $(\frac{G_F}{G_f})$
Small	10.31	3.04
Medium	9.096	2.68
Large	6.86	2.02

Brittleness number as defined [22] $\beta = \frac{d}{d_0}$ characterizes the brittleness of the member. According to Bazant [22] brittleness with $0.1 < \beta < 10$, the nonlinear fracture mechanics should be used. Quasi-brittle structures are those for which $0.1 \leq \beta \leq 10$ [25]. If $\beta < 0.1$, then the failure may be analyzed on the basis of the strength criterion and if $\beta > 10$, then the failure may be analyzed according to the linear elastic fracture mechanics [22]. Brittleness number for different sizes of specimens in the study are evaluated and are presented in the Table 8.

Table 8: Size Effect Law Data

Specimen type	$Log(\frac{d}{d_0})$	$Log(\frac{\sigma_N}{Bf_t})$	β
Small	-0.35	-0.08775	0.356
Medium	-0.051	-0.1775	0.711
Large	0.2499	-0.224	1.422

The values of brittleness number for small specimens are low when compared to large specimens which implies higher ductility for smaller specimens of UHPFRC. It was also observed that all the specimens have the brittleness value between 0.1 and 10 which validates the applicability of non linear fracture mechanics.

5 CONCLUSIONS

The following conclusions are drawn based on the present experimental study:

Steel fibers lead to nominal increase in compressive strength and marginal increase to tensile strengths in UHPC. Peak load, displacement and CMOD values increases with the increase in size of specimen for UHPFRC. It have

been observed that the energy absorption capacity much higher in UHPFRC as compared to normal concrete. Increase in the size of the structures increases the brittleness of the member.

REFERENCES

[1] Schmidt, M., & Fehling, E. (2005). Ultra-high-performance concrete: research, development and application in Europe. *ACI Special publication*, **228**, 51-78.

[2] Rokugo, K., Kanda, T., Yokota, H., & Sakata, N. (2007, July). Outline of JSCE recommendation for design and construction of multiple fine cracking type fiber reinforced cementitious composite (HPFRCC). *In Proceedings of the 5th International Conference on High Performance Fiber Reinforced Composites (HPFRCC5)* (pp. 10-13).

[3] Bhowmik, S., and Ray, S. (2019). An experimental approach for characterization of fracture process zone in concrete. *Engineering Fracture Mechanics*, **211**, 401-419.

[4] Stang, H., & Li, V. C. (2004). Classification of fiber reinforced cementitious materials for structural applications.

[5] Sobuz, H. R., Visintin, P., Ali, M. M., Singh, M., Griffith, M. C., & Sheikh, A. H. (2016). Manufacturing ultra-high performance concrete utilising conventional materials and production methods. *Construction and Building materials*, **111**, 251-261.

[6] Choi, J. I., Lee, B. Y., Ranade, R., Li, V. C., & Lee, Y. (2016). Ultra-high-ductile behavior of a polyethylene fiber-reinforced alkali-activated slag-based composite. *Cement and Concrete Composites*, **70**, 153-158.

[7] Lee, B. Y., Cho, C. G., Lim, H. J., Song, J. K., Yang, K. H., & Li, V. C. (2012). Strain hardening fiber reinforced alkali-activated mortar–a feasibility study. *Construction and Building Materials*, **37**, 15-20.

[8] Graybeal, B. A. (2006). Material property characterization of ultra-high performance concrete (No. FHWA-HRT-06-103). *United States. Federal Highway Administration. Office of Infrastructure Research and Development.*

[9] Richard, P., & Cheyrezy, M. H. (1995). Reactive powder concrete. *Cement and Concrete Research*, **25(7)**, 1501-1511.

[10] Aziz, O. Q., & Ahmed, G. H. (2012, September). Mechanical Properties of Ultra High Performance Concrete (UHPC). *In Twelfth International Conference on Recent Advances in Concrete Technology and Sustainability Issues* (pp. 1-16).

[11] Magureanu, C., Sosa, I., Negrutiu, C., & Heghes, B. (2010). Physical and mechanical properties of ultra high strength fiber reinforced cementitious composites. *Fracture Mechanics of Concrete and Concrete Structures*, Korea Concrete Institute, 1497-1491.

[12] Park, S. H., Kim, D. J., Ryu, G. S., & Koh, K. T. (2012). Tensile behavior of ultra high performance hybrid fiber reinforced concrete. *Cement and Concrete Composites*, **34(2)**, 172-184.

[13] Yoo, D. Y., Park, J. J., Kim, S. W., & Yoon, Y. S. (2013). Early age setting, shrinkage and tensile characteristics of ultra high performance fiber reinforced concrete. *Construction and Building Materials*, **41**, 427-438.

[14] Kang, S. T., Lee, Y., Park, Y. D., & Kim, J. K. (2010). Tensile fracture properties of an Ultra High Performance Fiber Reinforced Concrete (UHPFRC) with steel fiber. *Composite Structures*, **92(1)**, 61-71.

[15] Habel, K., Viviani, M., Denarié, E., and Brühwiler, E. (2006). Development of the mechanical properties of an ultra-high performance fiber reinforced concrete (UHPFRC). *Cement and Concrete Research*, **36(7)**, 1362-1370.

[16] Kazemi, S., & Lubell, A. S. (2012). Influence of Specimen Size and Fiber Content on Mechanical Properties of Ultra-High-Performance Fiber-Reinforced Concrete. *ACI materials Journal*, **109(6)**.

[17] Su, Y., Li, J., Wu, C., Wu, P., and Li, Z. X. (2016). Effects of steel fibres on dynamic strength of UHPC. *Construction and Building Materials*, **114**, 708-718.

[18] Rossi, P., Arca, A., Parant, E., and Fakhri, P. (2005). Bending and compressive behaviours of a new cement composite. *Cement and Concrete Research*, **35(1)**, 27-33.

[19] Bazant, Z. P., and Planas, J. (1997). *F*racture and size effect in concrete and other quasibrittle materials (Vol. 16). CRC press.

[20] Funk, J. E., and Dinger, D. R. (2013). Predictive process control of crowded particulate suspensions: applied to ceramic manufacturing. *Springer Science and Business Media*.

[21] Shah, S. P. (1990). Size-effect method for determining fracture energy and process zone size of concrete. *Materials and Structures*, **23(6)**, 461-465.

[22] Bazant, Z. P., and Kazemi, M. T. (1990). Determination of fracture energy, process zone longth and brittleness number from size effect, with application to rock and conerete. *International Journal of fracture*, **44(2)**, 111-131.

[23] IS-516. 1999. Methods of tests for strength of concrete. *Bureau of Indian Standards*, New Delhi.

[24] RILEM TC QFS (2004). Quasibrittle fracture scaling and size effect—Final report.*Mater. Struct*, **Vol.37**, pp.547-586.

[25] Nallathambi, P., and Karihaloo, B. L. (1986). Determination of specimen-size independent fracture toughness of plain concrete. *Magazine of Concrete Research*, **38(135)**, 67-76.

[26] Duan, K., Hu, X., and Wittmann, F. H. (2007). Size effect on specific fracture energy of concrete. *Engineering Fracture Mechanics*, **74(1-2)**, 87-96.